Volume 299, number 2, 135–142 FEBS 10786 March 1992

β-Lactamase TEM1 of *E. coli*

Crystal structure determination at 2.5 Å resolution

C. Jelsch[a,b], F. Lenfant[c], J.M. Masson[c] and J.P. Samama[a]

[a]*Laboratoire de Cristallographie Biologique, IBMC du CNRS, 15 rue René Descartes, 67084 Strasbourg Cedex, France,* [b] *Biostructure S.A., Les Algorithmes, Euclide, Parc d'Innovation, 67400 Ill Kirch-Graffenstaden, France* and [c]*INSA, Centre de Transfert en Biotechnologie et Microbiologie, Laboratoire d'Ingéniérie des Protéines, UA544 du CNRS, Avenue de Rangueil, 31077 Toulouse Cedex, France*

Received 23 December 1991; revised version received 15 January 1992

The crystal structure of β-lactamase TEM1 from *E. coli* has been solved to 2.5 Å resolution by X-ray diffraction methods and refined to a crystallographic R-factor of 22.7%. The structure was determined by multiple isomorphous replacement using four heavy atom derivatives. The solution from molecular replacement, using a polyalanine model constructed from the C_α coordinates of *S. Aureus* PC1 enzyme, provided a set of phases used for heavy atom derivatives analysis. The *E. coli* β-lactamase TEM1 is made up of two domains whose topology is similar to that of the PC1 enzyme. However, global superposition of the two proteins shows significant differences.

β-lactamase; Antibiotic resistance; X-ray structure; *E. coli*

1. INTRODUCTION

β-lactam antibiotics such as penicillins and cephalosporins have a lethal effect on bacteria through the acylation of the active site serine of DD-carboxypeptidases, essential enzymes in cell wall synthesis. β-lactamases constitute a family of enzymes that confer resistance towards β-lactam antibiotics by hydrolysing them into inactive compounds. The antibiotics resistance is in constant evolution and the knowledge of several three dimensional structures of β-lactamases is desirable in order to establish a correlation between substrate specificities, sequences and structure variations of proteins from various sources. In addition, the understanding of the catalytic mechanism of β-lactamases would be an important step in the design of improved β-lactam antibiotics or inhibitors of β-lactamase.

On the basis of their primary structures, β-lactamases were divided into four classes A, B, C [1] and D [2]. Enzymes from class A, C and D, the most commonly encountered, are serine hydrolases. Class B β-lactamases which contain a zinc cofactor are clearly distinct from the other enzymes [3]. The three-dimensional structures of three class A β-lactamases have been recently solved by X-ray crystallography: PC1 from *Staphylococcus Aureus* [4] and 749/C from *Bacillus licheniformis* [5,6] were refined to 2 Å resolution, that of *Streptomyces albus* G to 3 Å resolution [7]. These class A enzymes, of molecular weight 29000 Da, have similar structures [5].

Class C β-lactamase (39,000 Da) from *Citrobacter freundii* has been presented to 2 Å resolution [8]. Despite low sequence homology and higher molecular weight, its three-dimensional structure is closely related to those of class A β-lactamases and that of the *Streptomyces* R61 DD-carboxypeptidase [9]. These structural similarities emphasize the hypothesis of a common gene ancestor for all β-lactam target enzymes [10,11].

The plasmid mediated *E. coli* TEM1 enzyme is the most frequently encountered in Gram-negative clinical isolates and early attempts to solve its three-dimensional structure lead to a 5.5 Å resolution electron density map [12]. We carried out the present study in order to understand the structural effects of ponctual mutations that change the substrate profile of the enzyme and which result in naturally occuring proteins known as TEM2 to TEM9 [13]. High-resolution structure determination of the recombinant wild type enzyme is a mandatory step in a program combining site-directed mutagenesis and structural work designed to provide the structure–function relationships [14]. Preliminary crystallographic data were presented in a previous paper [15].

Abbreviations: PCMBS, *p*-chloromercury benzene sulfonic acid; INDEL, insertion and deletion.

Correspondence address: J.P. Samama, Laboratoire de Cristallographie Biologique, IBMC, 15 rue René Descartes, F-67084 Strasbourg Cedex, France. Fax: (33) (88) 61 06 80.

2. MATERIALS AND METHODS

2.1. *Crystallization and native data collection*

The enzyme is the product of the ampicillin-resistance gene carried on plasmid pBR322 in *E. coli*; the sequence differs from TEM1 β-lactamase by the two mutations V84I and A184V. Crystals with dimensions 0.5×0.4×0.4 mm^3 were grown using the hanging drop method in the presence of ammonium sulfate as precipitating agent. Purification of the protein and crystallization conditions have been described [15].

The crystals belong to the orthorhombic space group $P2_12_12_1$ with cell parameters: a= 43.1 Å, b= 64.4 Å, c= 91.2 Å and diffract to 1.75 Å. There is one molecule per asymmetric unit and the unit volume to molecular weight ratio is of 2.26 $Å^3$/Da. Diffraction data were collected to 1.8 Å resolution (Table I). Each crystal data set was processed using the Xengen software [16]. Intensity measurements were merged and scaled using the programs Rotavata and Agrovata of the CCP4 package from Daresbury laboratory, England.

2.2. *Molecular replacement*

A model was constructed from the 2.5 Å C_α coordinates of the *Staphylococcus aureus* PC1 β-lactamase (Protein Data Bank entry: 1BLM), [17] in the following way. The C_α tracing was divided into fragments according to the observed secondary structure pattern. The DGNL option of Frodo [18] was used to search, in a dictionary of known protein structures, for pieces of polypeptide chains which fit best each of these C_α fragments. The selected polypeptide fragments thus obtained were fused to build up a continuous polypeptide chain. The TEM1 amino acid sequence was introduced, bad contacts were removed manually and energy minimization was performed using the GROMOS program [19]. However the model structure used for molecular replacement was the corresponding polyalanine, with atomic B-factors of 20 $Å^2$ applied to all atoms, except those belonging to loop regions for which the B value was 60 $Å^2$.

Rotation functions were calculated using the Crowther's fast rotation function [20] with normalized structure factors at different resolution ranges. The Crowther and Blow translation function [21] TSFGEN implemented in the CCP4 package by Tickle [22] was performed on normalized structure factors between 4–20 Å resolution. In order to strengthen the translation function signal, a set of rotations differing by ±3° in α, β and γ were tried around the average rotation function solution. The twenty-first translation peaks were inspected on a computer graphics for crystal packing constraints. A dozen acceptable translations, were kept. Rigid body refinement was applied on each of them using the program CORELS [23] in order to find the true translation.

The correctly oriented polyalanine model was then subjected to further refinement with CORELS. After inclusion of all side-chain atoms, each α-helix, β-strand and coil was allowed to move independently with restraints at the cleavage sites. The refinement was continued with energy minimisation using X-PLOR [24] in the resolution range 3.5–10 Å (R-factor: 39%).

2.3. *Multiple isomorphous replacement and solvent flattening*

Heavy atom derivatives were prepared by adding to the protein crystal mother liquor a solution of heavy atom salts. Four heavy atoms derivatives were obtained: K_2PtCl_4, $KAu(CN)_2$, K_2HgI_4 and PCMBS (Table II). Heavy atom sites were identified from difference Fourier maps between derivative and native data using the molecular replacement solution phases and from inspection of the three Harker sections of the difference Patterson maps. Heavy atom positions, occupancies and B-factors were refined with the programs REFINE2 implemented in the CCP4 package and HEAVY [25]. Minor sites were displayed by Fourier residual maps. MIR phases were computed using the program PHARE in CCP4.

Solvent flattening techniques implemented in the RMOL package [26] were iteratively applied in order to improve the MIR phases [27]. The molecular replacement model, roughly corrected according to the 3.5 Å MIR map, was used to define the molecular envelope obtained by defining 4 Å radius spheres around Cα and Cβ atoms. The solvent content was 31% of the unit cell volume. Six cycles of solvent flattening were applied on the 4 Å MIR map. The improved phases were used for a new refinement of the heavy atoms parameters using the option 'PHASE' of program REFINE2. The new MIR maps were then modified by 6 cycles of solvent flattening, extending the resolution from 4 Å to 3.5 Å.

2.4. *Model building and refinement*

The electron density maps were displayed on an Evans and Sutherland graphic display (ESV 3+) and model manipulation was made using the program FRODO [17], adapted by Phil Evans. Crystallographic refinement was performed using the X-PLOR package [24]. Atomic B-factors were maintained at 11 $Å^2$. Molecular dynamics calculations were run using the slowcooling protocol for 2.7 ps (time step of 0.0005 ps) with decreasing temperature from 3000 K to 300 K [28].

2.5. *Sequence alignment*

The program ALIGN, from the N.I.H. sequence analysis package [29] was used for sequence alignments.

3. RESULTS AND DISCUSSION

3.1. *Structure determination*

The rotation function signal was very dependant upon the resolution range and inclusion of the low resolution data was necessary in order to get the right solution as a clear peak of the rotation function. The signal was best observed using data between 3.5 and 20 Å resolution and was lost when the resolution range was too narrow, e.g. 3.5–8 Å or 5–10 Å. Depending on the

Table I
Statistics on X-ray data collection for the native enzyme

Crystal	1	2	3	4	5	Merged
No. observed reflexions	28,260	23,500	15,700	126,100	58,200	251,700
No. independant reflexions	7,700	12,100	8,000	24,300	23,100	28,700
Max. resolution Å	2.5	2.1	2.1	1.75	1.75	1.8
R_{sym} (I) (%)	4.6	5.7	4.6	5.8	4.8	6.4

Completion of data at 1.8 Å: 98%. X-ray generator: rotating Cu anode. Power: 40 kV, 40–100 mA. Graphite monochromator. Siemens/Nicolet area detector. Distance crystal-detector: 10 or 12 cm helium path. Oscillation steps : 0.2°. Temperature of crystal during data collection: T=−4°C.

$$R_{sym}(I) = \Sigma|I-\langle I\rangle|/\Sigma|I|, \quad I = \text{intensity}$$

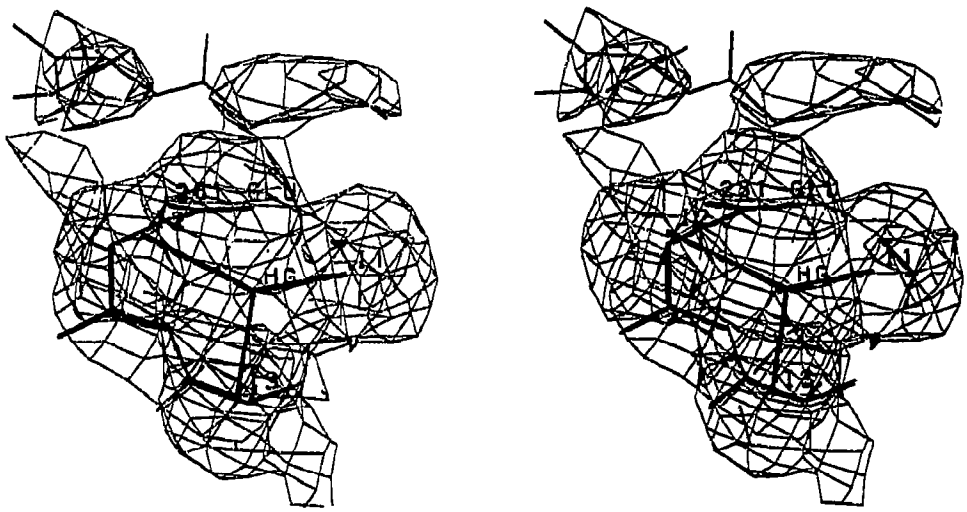

Fig. 1. Electron density map displaying the HgI_3^- main binding site.

resolution range, the rotation peak was found within 4° of the correct values: $\alpha = 171°$, $\beta = 75°$, $\gamma = 168°$.

The signal for the translation function search was always weak (0.5 sigma). The correct translation was not always in first position when different rotations around the average rotation were tried, but it was the most frequent. Rigid body refinement was necessary to identify the right solution and the correlation coefficient between calculated and observed structure factors proved to be very discriminative.

After partial refinement, this model met our requirements, in providing a set of initial phases whose quality allowed the initial interpretation of the heavy atom derivatives used to solve the structure (Table II). $PtCl_4^{2-}$ was of the least quality, with a phasing power which did not extend beyond 5 Å resolution. It reacted at two sites which were identified, from structure inspection, as methionines 129 and 272. $Au(CN)_2^-$ was of high quality with a good isomorphism up to 2.6 Å resolution. The negatively charged gold cyanide ions were found in the vicinity of lysine 34 and arginines 93 and 61. The two other derivatives, PCMBS and HgI_4^{2-}, were of medium quality. One PCMBS molecule reacted with histidine 112 and a second one was found in the catalytic cavity. HgI_4^{2-} is known to dissociate in solution into a mixture of HgI_3^-, HgI_2 and I^- depending upon the halide ion concentration [30]. The equilibrium is driven towards the formation of HgI_3^- as major ion species in the presence of potassium iodide [31]. We thus used two equivalents of potassium iodide for one K_2HgI_4. A difference Fourier map at 3.1 Å resolution showed, at the major binding site, a tetraedral shape electron density (Fig. 1). A mercury atom was placed at its center and iodine atoms in three of the electron density bumps. The fourth ligand of the mercury atom may be provided by the carboxylate group of glutamic acid 282. The above as-

Table II
Heavy atom derivatives: data collection and refinement

	K_2PtCl_4	$KAu(Cn)_2$	K_2HgI_4	PCMBS
Soaking conditions (mM)	2	4	2	7
(days)	2	7	5	8
No. independant reflexions	2,830	11,900	4,300	4,240
No. measured reflexions	14,700	87,600	25,100	16,900
$R_{sym}(I)$ (%)	7.6	5.8	9.8	6.5
$R_{iso}(F)$ (%)	15.9	11.8	29.7	11.1
Number of sites	2	1	2	2
Limit of isomorphism (Å)	5	2.6	3.1	3.1
Centric Cullis R-factor (%)	77	46	61	70
Phasing power	1.7	2.4	1.5	1.6

$R_{iso}(F) = \Sigma|F_{PH} - F_P| / \Sigma|F_P|$, F = structure factor.
Cullis R-factor: $\Sigma|(F_{PH} - F_P) - F_H| / \Sigma|F_{PH} - F_P|$
Phasing power: F_H / Lack of closure

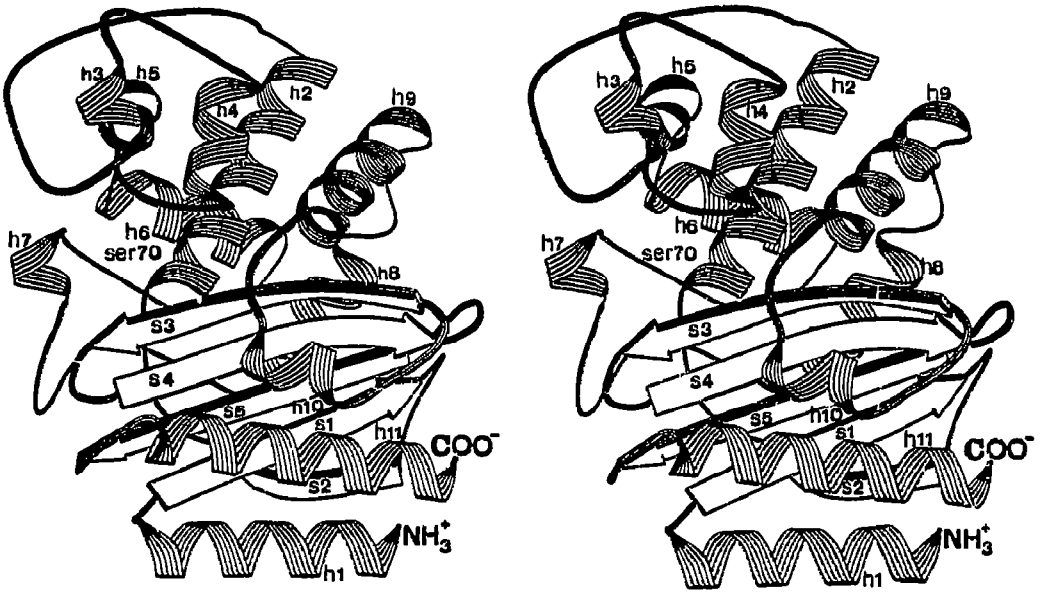

Fig. 2. Ribbon representation of the three-dimensional structure of the TEM1 β-lactamase.

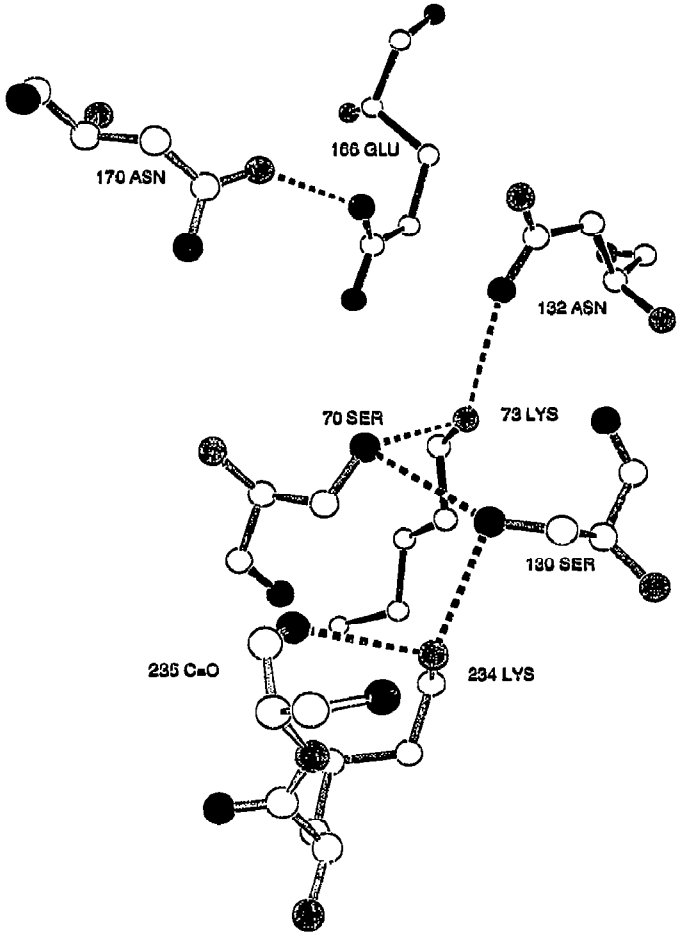

Fig. 3. Hydrogen bond network in the catalytic cavity.

signment led to excellent correlations on centric reflexions between observed and calculated heavy atom structure factors.

Solvent flattening resulted in a noticeable lowering of the noise in the initial MIR map and to an improvement of the electron density for side chains. The 3.5 Å solvent flattened M.I.R. map with coefficients F_{obs} x m_{MIR} allowed unambiguous mainchain tracing except in loops 87–92, 157–159, 254–258 and 274–276. The electron densities for side chains were defined except for 40 residues which were treated as alanines in the first reciprocal space refinement cycle performed between 8 and 2.9 Å resolution (final R-factor: 34%). Complete assignment of the protein electron density was done in a $F_{obs} \times m_{comb}$ map using combined phases [32] at 2.9 Å resolution. Combination of the M.I.R. and calculated phases led, indeed, to the best electron density map at this stage. The R factor after refinement was 26%. A few corrections were done (main chain, carbonyl atoms and side chains) in a $(3F_{obs}-2F_{calc}, \Phi_{calc})$ electron density map computed between 12–2.5 Å. The last refinement

Table III

Resolution range	No. Reflexions	R-factor (%)
8.0–4.7	1,165	26.2
4.7–3.8	1,131	17.6
3.8–3.4	1,120	20.0
3.4–3.1	1,111	22.4
3.1–2.9	1,103	23.7
2.9–2.7	1,114	25.4
2.7–2.6	1,081	25.2
2.6–2.5	1,094	24.9

R-factor as a function of resolution

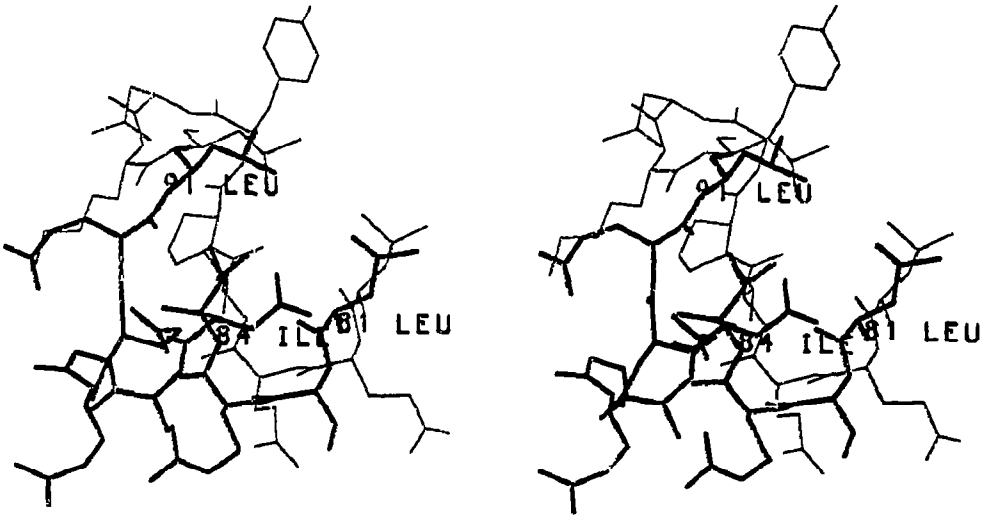

Fig. 4. Stereo view of the loop Leu[81]–Leu[91], located after helix h2. TEM1 (thick lines), PC1 (thin lines).

cycle between 8–2.5 Å led to an R-factor of 22.7% (Table III). The mean B-factor is 6.2 Å^2 for main-chain atoms and 9.8 Å^2 for side-chain atoms.

3.2. *General description*

The 263 residues of TEM1 are assigned according to the Ambler numbering of class A β-lactamases [1]. A schematic representation of the three-dimensional structure of TEM1 is shown in Fig. 2. The protein is made of two domains closely packed together. The first one is build up from five antiparallel strands. One side of the sheet is shielded from the solution by the N- and C-terminal helices (h1, h11) and by helix h10. The second domain, residues 61–211, is made of 8 helices essentially connected by loops. Two short sheets (not indicated on Fig. 2) are found in this domain. They are made of respectively 2 and 3 antiparallel strands of 2–3 residues. Cysteine 77 at the C-terminal end of helix h2 and cysteine 123 on helix h4 form a disulfide bridge. The *cis* peptide bond between Glu[166] and Pro[167], described in the PC1 enzyme [4], is also present in TEM1. These residues belong to the Ω loop (residues 163–178, including the short helix h7) [4] which delimitates the active site region towards the solution. The active site cavity forms part of the interface between the two domains. All residues implicated in catalysis are intricated in a hy-

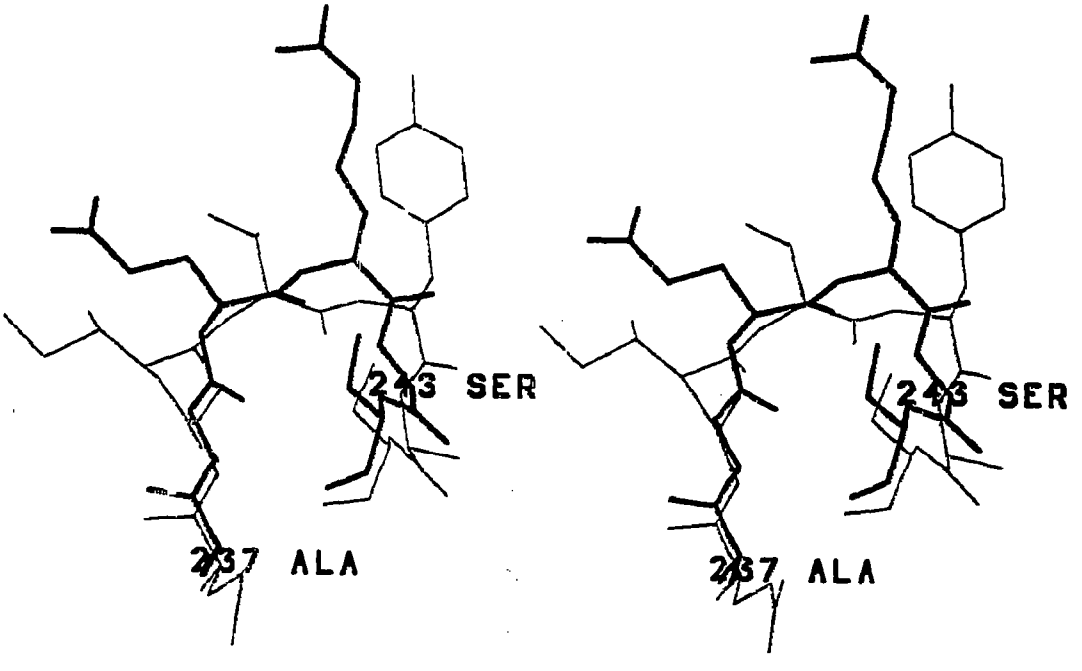

Fig. 5. Stereo view of the loop Ala237-Ser243, connecting strands s3 and s4. TEM1 (thick lines), PC1 (thin lines).

Table IV A
Sequence alignment

```
          26  30   35   40   45   50   55   60   65   70   75   80
TEM1       HPETLVKVKDAEDQLGARVGYIELDLNSGKILESFRPEERFPMMSTFKVLLCGAVLSRVD
PC1        -----KELNDLEKKYNAHIGVYALDTKSGKEVK-FNSDKRFAYASTSKAINSAILLEQVP

          86  90   95  100  105  110  115  120  125  130  135  140
TEM1       AGQEQLGRRIHYSQNDLVEYSPVTEKHLTDGMTVRELCSAAITMSDNTAANLLLTTIGGP
PC1        YNK--LNKKVHINKDDIVAYSPILEKYVGKDITLKALIEASMTYSDNTANNKIIKEIGGI

         146 150  155  160  165  170  175  180  185  190  195  200
TEM1       KELTAFLHNMGDHVTRLDRWEPELNEAIPNDERDTTMPAAMATTLRKLLTGELLTLASRQ
PC1        KKVKQRLKELGDKVTNPVRYEIELNYYSPKSKKDTSTPAAFGKTLNKLIANGKLSKENKK

         206 210  215  220  225  230  235  240  245  250  255  260  265
TEM1       QLIDWMEADKVAGPLLRSALPAGWFIADKSG-AGERGSRGIIAALGPDGKPSRIVVIYTT
PC1        FLLDLMLNNKSGDTLIKDGVPKDYKVADKSGQAITYASRNDVAFVYPKGQSEPIVLVIFT

         266 270  275  280  285  290
TEM1       GSQATMDERNRQ-IAEIGASLIKHW
PC1        NKDNKSDKPNDKLISETAKSVMKEF
```

TEM1, β-lactamase from *E. coli*; PC1, β-lactamase from *S. aureus*.

drogen bond network (Fig. 3). The essential Ser^{70} side chain is at the N-terminal part of helix h2 and at hydrogen bond distance to both Lys^{73} and Ser^{130}. Lys^{234} amino group is within hydrogen bond distance to Ser^{130} side chain and to Ser^{235} main-chain carbonyl oxygen. This lysine 234 was shown by site-directed mutagenesis to be directly involved in substrate binding [33,34]. Glu^{166} forms a salt bridge with Lys^{73}; it may act as an acid/base catalyst in the hydrolysis of the β-lactam ring and seems involved in, at least, the deacylation step [35–37]. Its replacement by alanine, asparagine or glutamine led to a stable acyl-enzyme with benzylpenicillin as substrate. Surprisingly, the E166Y mutant protein was shown, to be as efficient towards cephalosporins and penicillins [36]. Complete description of the protein should however await structure refinement at 1.8 Å resolution and inclusion of the water molecules.

3.3. *Structure superposition and sequence alignment of the TEM1 and PC1 enzymes*

The three-dimensional superposition of both proteins has been achieved using a least-square minimisation algorithm. The C_α positions from both proteins have been used except those corresponding to INDEL regions: 26–30, 51–57, 84–90, 239–241, 251–257 for which visual inspection clearly showed large differences. Despite identical folding of the PC1 and TEM1 enzymes, the R.M.S. value, after superposition of the least

Table IV B
Amino acid correspondance from X-ray structure superposition

```
          26  30   35   40   45   50   55   60   65   70   75   80
TEM1       HPETLVKVKDAEDQLGARVGYIELDLNSGKILESFRPEERFPMMSTFKVLLCGAVLSRVD
PC1        -----KELNDLEKKYNAHIGVYALDTKSGKE-VKFNSDKRFAYASTSKAINSAILLEQVP

          86  90   95  100  105  110  115  120  125  130  135  140
TEM1       AGQEQLGRRIHYSQNDLVEYSPVTEKHLTDGMTVRELCSAAITMSDNTAANLLLTTIGGP
PC1        YNK--LNKKVHINKDDIVAYSPILEKYVGKDITLKALIEASMTYSDNTANNKIIKEIGGI

         146 150  155  160  165  170  175  180  185  190  195  200
TEM1       KELTAFLHNMGDHVTRLDRWEPELNEAIPNDERDTTMPAAMATTLRKLLTGELLTLASRQ
PC1        KKVKQRLKELGDKVTNPVRYEIELNYYSPKSKKDTSTPAAFGKTLNKLIANGKLSKENKK

         206 210  215  220  225  230  235  240  245  250  255  260  265
TEM1       QLIDWMEADKVAGPLLRSALPAGWFIADKSGAGERG SRGIIAALGP DGKPSRIVVIYT
PC1        FLLDLMLNNKSGDTLIKDGVPKDYKVADKSGQAITYASRNDVAFVYPKGQSEPIVLVIFT
                                                ^^^^          ^^^^^

         266 270  275  280  285  290
TEM1       TGSQATMDERNRQIAEIGASLIKHW
PC1        NKDNKSDKPNDKLISETAKSVMKEF
```

TEM1, β-lactamase from *E. coli*; PC1, β-lactamase from *S. aureus*; ^^^^, indicates the loop regions where deletions occur in the TEM1 enzyme.

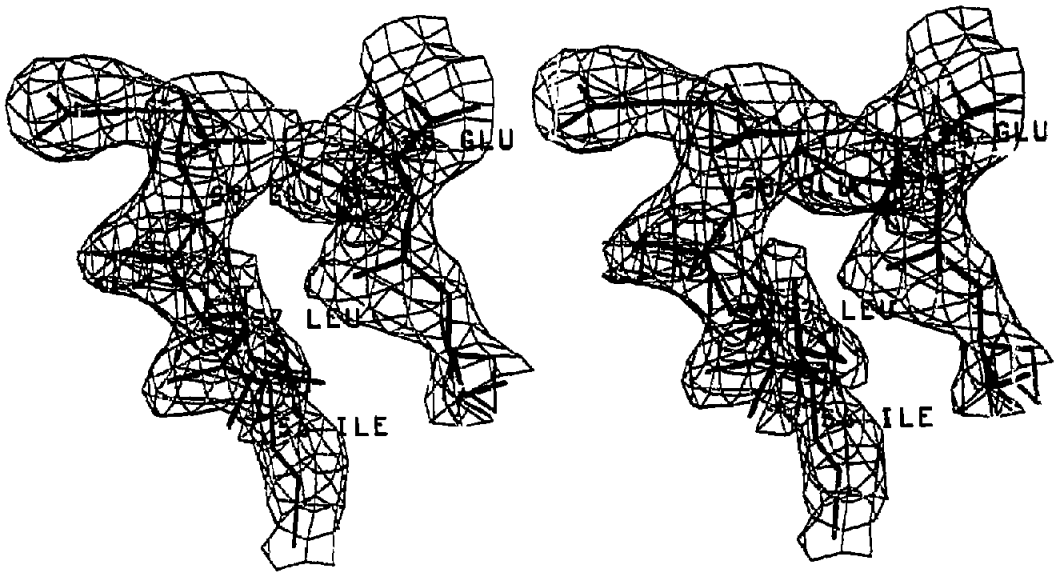

Fig. 6. Stereo view of the electron density map in the β-bulge region.

differing C_α chain tracing, is high (2.16 Å) and illustrates that significant differences occur. They may arise from the non-conserved sequence regions and will require further detailed analysis.

The sequence alignment (Table IVA) suggests that Ser[59], Glu[89] and Gln[90] found in the TEM1 enzyme are deleted in the PC1 enzyme, whereas Gln[237] and Leu[278] in PC1 are absent in TEM1. It should be mentioned that other sequence alignment programs [38] led to slightly different INDEL locations. After superposition of the C_α atoms from both X-ray structures, the INDEL regions were located and analysed. The resulting sequence alignment is given in Table IVB. Except for Glu[89] and Gln[90], found at the C-terminal end of the h2 helix, in a loop which differs significantly in the two enzymes (Fig. 4), the INDEL locations are not in agreement with the sequence alignment (Table IVA and IVB). The most striking difference is about the proposed deletion at position 278 in TEM1 which actually occurs in the region 252–257 in the loop connecting the antiparallel strands s4 and s5. From sequence alignment, one amino acid deletion was expected at the important position 237 (position 239 in ref. [38]), on β-strand s3 in the vicinity of the active site. It however turns out that this deletion does not affect the overall topology and occurs in the connection between strands s3 and s4. This short loop is made of three residues in TEM1 (Glu, Arg, Gly) and of four residues in PC1 (Ile, Thr, Tyr and Ala). The residues from both proteins which are nearly superimposed at the edge of the loop are respectively for TEM1 and PC1: Ala and Gln at 237, Ser and Ser a 243 (Fig. 5). Compared to PC1, a leucine residue is insorted at position 57 in the TEM1 structure. This residue is part of strand s2, at the solvent interface. The two protein structures display significant differences in this area, and it appears that this insertion is accomodated through the formation of a β-bulge between strands s1 and s2. According to the classical bulge nomenclature, Leu[57], Glu[58] and Glu[48] are respectively at positions 1, 2 and X of that motif (Fig. 6). The N-terminus helix is five residues longer in the TEM1 enzyme. When the protein X-ray structures are superimposed as described above, the N-terminal helices of TEM1 and PC1 show a global displacement corresponding to about half a helix turn.

3.4. *Specific residues for Gram negative β-lactamases*

A sequence alignment made on eight class A β-lactamases [38] pointed out some residues (245, 246, 251) that are conserved among the six Gram positive enzymes, but not in the two Gram negative sub-groups: TEM1 and LEN1. Asparagine at position 245 in PC1 is a glycine in TEM1. The empty space thus created is occupied by a methionine 69 side chain, which replaces the corresponding alanine in PC1. The environment of the aspartic acid 246 in the Gram positive β-lactamase PC1 from *S. Aureus* was described by Herzberg [4]. This buried carboxylate group is replaced in TEM1 by a hydrophobic isoleucine. This residue is pointing into a large hydrophobic cluster between the main β sheet and helices h1, h10 and H11. Tyrosine 251 in PC1 is a glycine in TEM1. This residue is located at the C-terminal end of strand s4. This mutation is compensated in TEM1 by the K230F mutation at the N-terminal end of strand s3, the hydrophobic side chain pointing toward the core of the protein.

The refinement of the TEM1 structure will be pursued to 1.8 Å resolution. Location of the water molecules, detailed analysis of the structure and X-ray structure analysis of ponctual mutants should provide

insights into the structure–function relationships and about the differences between this protein and the known structures of other β-lactamases.

Acknowledgements: We thank D. Moras for facilities placed at our disposal and for his interest in this project. This work was supported in part by the French Ministry of Research and Technology (contract no. 89T0840).

REFERENCES

[1] Ambler, R.P. (1980) Phil. trans. Res. Soc. B 289, 321–331.
[2] Joris, B., Ghuysen, J.M., Dive, G., Renard, A., Dideberg, O., Charlier, P., Frère, J.M., Kelly, J.A., Boyington, J.C., Moews, P.C. and Knox, J.R. (1988) Biochem. J. 250, 313–324.
[3] Sutton, B.J., Artymiuk, P.J., Cordero-Borboa, A.E., Littke, C., Phillips, D.C. and Waley, S.G. (1987) Biochem. J. 248, 181–188.
[4] Herzberg, O. (1991) J. Mol. Biol. 217, 701–719.
[5] Moews, P., Knox, J., Dideberg, O., Charlier, P. and Frère, J.M. (1990) Proteins 7, 156–171.
[6] Knox J.R. and Moews, P.C., (1991), J. Mol. Biol., 220, 435–455.
[7] Dideberg, O., Charlier, P., Wery, J.P., Dehottay, P., Dusart, J., Erpicum, T., Frère, J.M. and Ghuysen, J.M. (1987) Biochem. J. 245, 911–913.
[8] Oefner, C., d'Arcy, A., Daly, J.J., Gubernator, K., Charnas, R.L., Heinze, I., Hubschwerlen, C. and Winkler, F.K. (1990) Nature 343, 284–288.
[9] Kelly, J., Knox, J., Moews, P., Hite, G., Bartolone, J., Zhao, H. and Joris, B., Frère, J.M., Ghuysen, J.M. (1985) J. Biol. Chem. 260, 6449–6458.
[10] Kelly, J.A., Dideberg, O., Charlier, P., Wery, J.P., Libert, M., Moews, P., Knox, J., Duez, C., Fraipont, C.L., Joris, B., Dusart, J., Frère, J.M. and Ghuysen, J.M. (1986) Science 231, 1429–1431.
[11] Samraoui, B., Sutton, B.J., Todd, R.J., Artymiuk, P.J., Waley, S.G., Phillips, D.C. (1986) Nature 320, 378–380.
[12] Knox, J., Kelly, J., Moews, P., Murthy, N.S. (1976) J. Mol. Biol. 104, 865–875
[13] Collatz, E., Tran Van Nhieu, G., Billot-Klein, D., Williamson, R. and Gutmann, L. (1989) Gene 78, 349–354.
[14] Lenfant, F., Labia, R., Masson, J.M. (1990) Biochimie 72, 495–503.
[15] Jelsch, C., Lenfant, F., Masson, J.M. and Samama, J.P. (1992) J. Mol. Biol. 223, 377–380.
[16] Howard, A.J., Gilliland, G.L., Finzel, B.C., Poulos, T.L., Ohlendorf, D.H. and Salemme, F.R. (1987) J. Appl. Crystalogr. 20, 383–387.
[17] Herzberg, O. and Moult, J. (1987) Science 236, 694–701.
[18] Jones, T.A. and Thirup, S. (1986) EMBO J. 5, 819–822.
[19] van Gunsteren, W.F. and Berendsen, H.J.C. (1987) GROMOS, Groningen Molecular Simulation Library, BIOMOS b.v. Groningen, The Netherlands.
[20] Crowther, R.A. (1972) in: The Molecular Replacement Method, (Rossmann, M.G.) pp. 173–178, Gordon and Breach, New York.
[21] Crowther, R.A. and Blow, D.M. (1967) Acta Crystalogr. 23, 544–548.
[22] Tickle, I. (1985) Molecular replacement, Proceedings of the the Daresbury Study Weekend, 15–16 February 185, edited by P.A. Machin, pp. 22–26, Warrington: SERC Daresbury Laboratory.
[23] Sussmann, J.L., Holbrook, S.R., Church, G.M. and Kim, S.H. (1977) Acta Crystalogr. A33, 800–804.
[24] Brünger, A.T. (1990) X-PLOR Manual, v. 2.1., The Howard Hugues Medical Institute and Department of Molecular Biophysics and Biochemistry, Yale University, New Haven, USA.
[25] Terwilliger, T.C. and Eisenberg, D. (1987) Acta Crystalogr. A43, 6–13.
[26] Rees, B., Bilwes, A., Samama, J.P. and Moras, D. (1990) J. Mol. Biol. 214, 281–297.
[27] Bricogne, G. (1976) Acta Crystalogr. A32, 832–847.
[28] Brünger, A.T., Karplus, M. and Petsko, G.A. (1989) Acta Crystalogr. A45, 50–61.
[29] Pearson, W.R. and Lippman, D.J. (1988) Proc. Natl. Acad. Sci. 85, 2444–2448.
[30] Cotton, F.A. and Wilkinson, G. (1980) in: Advances in Inorganic Chemistry, p. 605, J. Wiley and sons, New York.
[31] Petsko, G. (1985) Methods Enzymol., 114, 147–156.
[32] Stuart, D. and Artymiuk, P. (1984) Acta Crystallogr. A40, 713–716.
[33] Ellerby, L.M., Escobar, W.A., Fink, A.L., Mitchinson, C. and Wells, J.A. (1990) Biochemistry 29, 5797–5806.
[34] Lenfant, F.L., Labia, R. and Masson, J.M. (1991) J. Biol. Chem. 15, 17187–17194.
[35] Adachi, H., Ohta, T. and Matsuzawa, H. (1991) J. Biol. Chem. 266, 3186–3191
[36] Delaire, M., Lenfant, F., Labia, R. and Masson, J.M. (1991) Protein Eng. 4, 805–810.
[37] Madgwick, P.J. and Waley, S.G. (1987) Biochem. J. 248, 657–662.
[38] Pastor, N., Pinero, D., Valdés, A.M. and Soberon, X. (1990) Molec. Microbiol. 4, 1957–1965.